Computational Fluid Dynamics Modeling of Ventilation of Confined-Space Manure Storage Facilities: Applications

J. Zhao, H. B. Manbeck, D. J. Murphy

ABSTRACT. *Fatalities associated with entry into on-farm confined-space manure storage tanks occur each year. The fatalities are due to asphyxiation or poisoning by exposure to high concentrations of hydrogen sulfide, methane, and carbon dioxide. Forced ventilation has been shown to be an effective way to reduce concentrations of these noxious gases to levels that are safe for human entry into these storage tanks. Hydrogen sulfide (H_2S) was used as an indicator gas to investigate the effectiveness of forced ventilation strategies for eliminating the toxic and oxygen-deficient atmospheres in confined-space manure tanks. Validated computational fluid dynamics (CFD) modeling protocols were used to simulate H_2S evacuation from fan-ventilated manure tanks. The simulation studies were conducted for rectangular and circular manure tanks, and the effects of pollutant source, inter-contamination (process by which a portion of exhausted contaminant gas enters a ventilated confined airspace through the fresh air intake), storage size (i.e., length, diameter), and air exchange rate on H_2S removal from fan-ventilated manure tanks were investigated. For the same air exchange rate, as the size (i.e., length, diameter) of the tank increased, the rate of evacuation of the H_2S from the confined space decreased. For rectangular and circular manure tanks, the higher the air exchange rate, the higher the rate of evacuation of the H_2S from the confined space. For the rectangular tank geometries and ventilation system layouts simulated, evacuation times decreased exponentially with air exchange rate. Evacuation times for the circular tanks simulated decreased linearly with air exchange rate.*

Keywords. *Air exchange rate, CFD modeling protocols, Confined-space manure storage facilities, Forced ventilation, Hydrogen sulfide, Simulation.*

The Occupational Safety and Health Administration (OSHA, 1998) definition of a confined space is one that: "(1) Is large enough and so configured that an employee can bodily enter and perform assigned work; (2) Has limited or restricted means for entry or exit; and (3) Is not designed for continuous employee occupancy." Many manure storage facilities are confined spaces, and entry into these confined spaces has been identified as a major safety concern (NIOSH, 1990). In confined-space manure storage facilities, toxic and/or explosive gases as well as oxygen-deficient atmospheres resulting from fermentation of the stored manure create very hazardous conditions to farmers who may need to enter these storage facilities to work or perform maintenance. The typical gases emitted from the manure include methane (CH_4), ammonia (NH_3), carbon dioxide (CO_2), and hydrogen sulfide (H_2S). Hydrogen sulfide was used as the indica-

Submitted for review in April 2007 as manuscript number JASH 6975; approved for publication by the Journal of Agricultural Safety and Health of ASABE in April 2008.

The authors are **Juan Zhao, ASABE Member,** PhD, Post-Doctoral Researcher, **Harvey B. Manbeck, ASABE Fellow,** PhD, Distinguished Professor Emeritus, and **Dennis J. Murphy, ASABE Member,** PhD, Distinguished Professor, Department of Agricultural and Biological Engineering, The Pennsylvania State University, University Park, Pennsylvania. **Corresponding author:** Harvey B. Manbeck, The Pennsylvania State University, 210 Agric. Engineering Bldg., University Park, PA 16802; phone: 814-865-4071; fax: 814-863-1031; e-mail: hmanbeck@psu.edu.

  ISSN 1074–7583

tor gas to measure the effectiveness of candidate ventilation strategies for eliminating the toxic and oxygen-deficient atmospheres in confined-space manure tanks, to validate computational fluid dynamics (CFD) modeling protocols for predicting the effectiveness of ventilation strategies for removing noxious gases from manure storage tanks, and to perform CFD simulations for typical on-farm confined-space manure tanks using the validated CFD modeling protocols.

The health and safety issues associated with confined-space manure storage facilities are well documented (e.g., CDC, 1993; NIOSH, 1990). The ailments and deaths related to the exposure of asphyxiating, as well as toxic, atmospheres in confined-space manure storage facilities are also documented. Fatalities associated with on-farm confined-space manure storage facilities frequently occurred when a victim entered an unventilated manure storage facility to make repairs or to perform maintenance without wearing the necessary personal protection equipment (PPE). Tragically, the accidents occurring in confined-space manure storage facilities often involve multiple fatalities when other poorly trained and equipped farm personnel attempted a rescue and became victims as well (Murphy and Steel, 2001). Beaver and Field (2007) summarized the documented fatalities in livestock manure storages and handling fatalities from 1975 to 2004. They found, from their analyses of 77 documented fatality cases, an increasing trend in the death rate per year between 1975 and 2004: 1.6 from 1975 through 1984, 2.7 from 1985 through 1994, and 3.5 from 1995 through 2004.

OSHA has developed confined-space regulations documented in Chapter 29 Part 1910.146 of the Code of Federal Regulations (CFR). These regulations are summarized in Permit-Required Confined Spaces (OSHA, 2002) and require that the internal atmosphere within a confined space be tested for oxygen levels, flammable gases and vapors, and potential noxious contaminants prior to human entry. Forced-air ventilation must be used when the gas concentrations exceed their permissible levels. According to OSHA standards, an employee may not enter a confined space until the forced-air ventilation has eliminated any existing hazardous atmosphere. However, research studies on safety ventilation in confined-space manure storage facilities are limited. Lloyd (2000) studied ventilation of a below-ground manure reception pit adjacent to a swine housing facility. In his research, airflow entry location and storage cover could not be adjusted. These limitations in Lloyd's research were overcome by Pesce et al. (2007), who used a rectangular, confined-space manure tank (dimension of confined airspace in the tank: $L \times W \times H = 5.49 \times 2.74 \times 1.83$ m) to identify the best ventilation strategies (fan location, outlet location) for each of three cover types: solid, fully slotted, and partially slotted. Alternative fan location, cover type, and airflow rate were also considered in Pesce's study (Pesce et al., 2007).

Computational fluid dynamics (CFD) modeling has been a useful tool for predicting air movement in ventilated spaces, including spatial variations in temperatures and pollutant concentrations (Sørensen and Nielsen, 2003). Zhao et al. (2007b) developed and validated CFD modeling protocols to simulate H_2S concentration decrease during forced ventilation for the best ventilation strategies identified by Pesce et al. (2007). They simulated the time taken to reduce H_2S concentration from initial concentration (C_0) to the OSHA permissible exposure limit (PEL-H_2S = 10 ppm; OSHA, 1995) (T_{pel}), the time taken to reduce H_2S concentration to 50% of the initial concentration (gas concentration at the beginning of the ventilation) (T_{50}), the time taken to reduce H_2S concentration to 25% of the initial concentration (T_{25}), and the time taken to reduce H_2S concentration to 10% of the initial concentration (T_{10}) in the entire confined airspace. An extended validation of the CFD modeling protocols was performed using an independent, underground manure reception pit adjacent to a mono-sloped, naturally ventilated swine growing and finishing barn at the Pennsylvania State University Swine Research Center

(Zhao et al., 2007b). The H_2S emission rates (from stored manure) and inter-contamination ratios (the ratio of contaminant concentration at the fan intake to the concentration in the air exhausted from manure storage facilities) obtained experimentally were important input parameters for the CFD simulations. Zhao et al. (2007a) conducted experimental measurements of H_2S emission rates and inter-contamination ratios using the manure tank used by Pesce et al. (2007). The emission rates were measured under typical forced ventilation airflow conditions for three temperature regimes (cold = $t < 13^{\circ}C$, mild = $13^{\circ}C < t < 18^{\circ}C$, and hot = $t > 18^{\circ}C$) for two air exchange (AC) rates (the rate at which outside air replaces indoor air in a space, AC min^{-1}) (high = 5 AC min^{-1} and low = 3 AC min^{-1}). The inter-contamination ratios were measured for typical forced ventilation conditions for storage facilities with solid, fully slotted, and partially slotted cover types. The CFD modeling protocols were validated based on comparisons between simulated and measured time values (i.e., T_{pel}, T_{50}, T_{25}, and T_{10}). Simulated and measured times within the confined-space manure storage facilities agreed to within 10% at all measuring locations except those immediately adjacent to the ventilation fan jet, at which corresponding times agreed within 15% in the high-velocity gradient region of the ventilation fan jet. The validated modeling protocols were recommended as efficient tools, in place of experimental measurements, for identifying effective ventilation strategies for evacuating noxious gases from on-farm, confined-space manure storage tanks.

This article presents initial applications of the validated CFD modeling protocols and identifies the effects of pollutant source (H_2S emission rates from manure), inter-contamination (process by which a portion of exhausted contaminant gas enters a ventilated confined airspace through the fresh air intake), air exchange rate in the confined airspace, and storage size (i.e., length, diameter) on contaminant gas removal from the confined airspace. These factors were identified by Zhao et al. (2007b) as potential influencing factors on gas evacuation during forced ventilation. The objective of this article is to quantify the effects of these factors on H_2S removal from the confined-space manure storage facilities based on results of simulations performed using the validated CFD modeling protocols. In order to ensure the conservativeness of results, the comparisons of T_{pel} or T_{25} values were conducted at the location in the area with the highest gas concentration.

Simulation Cases and Methodology

The most common on-farm confined-space manure storage tanks have either a rectangular or circular footprint. The tank's required storage volume is dependent upon the following factors: number of animal units, number of days of storage, wastewater volume, runoff volume, precipitation volume, and bedding volume (*ASAE Standards*, 2004); therefore, manure storage sizes are not standardized. The size and geometry of the manure storage tanks used to conduct simulation studies were based on typical aspect ratios (length/width) of rectangular tanks in swine facilities and typical heights and diameters of cylindrical tanks (MWPS, 1987). Table 1 lists the schedule of simulation studies. The width and depth of the rectangular manure storage tanks were kept the same as the rectangular manure tank used in previous research (Zhao et al., 2007a) (width = 2.74 m, height = 1.83 m). In these tanks, manure was stored at the bottom. Here, the height of the tank represents the distance from the top floor of the tank to the manure surface. The airspace depth of all the circular manure storage tanks simulated was 1.83 m, the same as for the rectangular manure tanks. The diameter of the simulated circular manure tanks was based on the equivalent volume of the simulated rectangular manure tanks.

Table 1. Simulation schedule.

Manure Storage	Floor Type	Storage Dimensions (m)	Volume (m^3)	Grid Density[a] ($X \times Y \times Z$)	Cell Volume (m^3)[b]		Air Exchange Rate (AC min^{-1})
					Fan Area	Outside Fan Area	
Rectangular (L×W×H)	Fully slotted	5.49×2.74×1.83	27.5	82×42×23	1.2×10^{-4}	1.3×10^{-3}	1, 3, 5
		12.2×2.74×1.83	61.2	116×32×24	1.9×10^{-4}	2.1×10^{-3}	1, 3, 5
		18.3×2.74×1.83	91.8	162×32×24	1.9×10^{-4}	2.1×10^{-3}	3
	Partially slotted	5.49×2.74×1.83	27.5	86×44×22	9.5×10^{-5}	1.4×10^{-3}	1, 3, 5
		12.2×2.74×1.83	61.2	126×34×20	1.9×10^{-4}	2.3×10^{-3}	1, 3, 5
		18.3×2.74×1.83	91.8	186×34×20	1.9×10^{-4}	2.3×10^{-3}	5
Circular (D×H)	Solid	4.4×1.83	27.8	44×42×18	2.8×10^{-4}	4.7×10^{-3}	3
		6.5×1.83	60.7	44×44×16	2.5×10^{-4}	2.1×10^{-3}	1, 3, 5

[a] Grid density represents the grid numbers in the *X*-, *Y*-, and *Z*-directions.
[b] Cell volume = volume of each control volume.

Simulations for the rectangular tanks were performed for the fully slotted and partially slotted cover types. For circular tanks, simulations were performed only for the solid cover type. Figure 1 shows the top view of the CFD domain for simulated tanks with rectangular (figs. 1a and 1b) and circular (fig. 1c) footprints. The domain was set up using a Cartesian coordinate system in the PHOENCIS (3.6) CFD code (CHAM, 2005). For the rectangular footprint with the fully slotted and partially slotted covers, the fan (air inlet area = 0.29 m^2) was located at the mid-point of the top floor of the manure tank. The

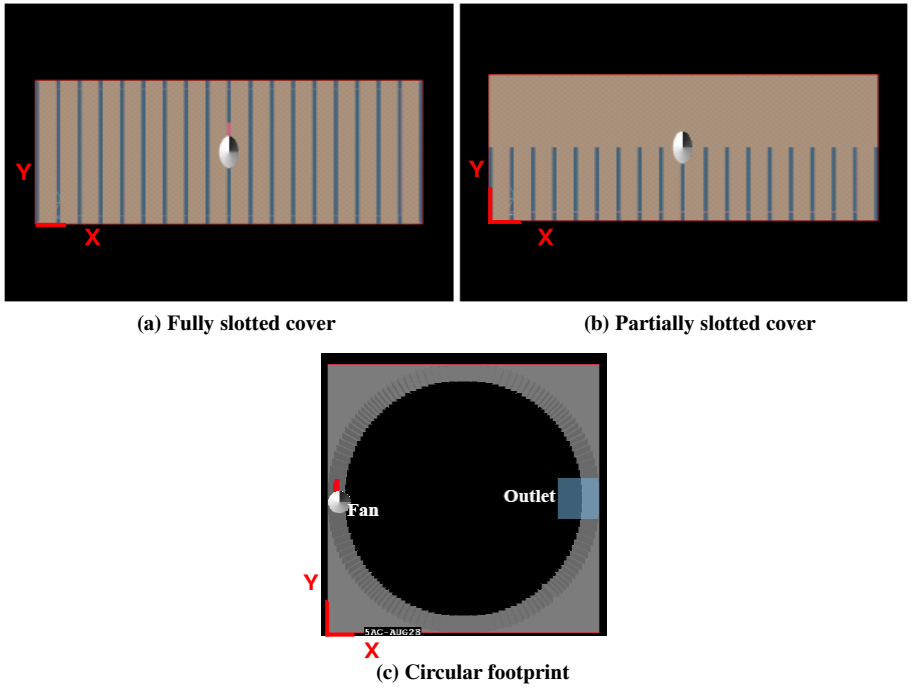

(a) Fully slotted cover **(b) Partially slotted cover**

(c) Circular footprint

Figure 1. Top view of CFD domain for rectangular manure tanks with (a) the fully slotted cover and (b) the partially slotted cover and for (c) circular manure tank with the solid cover (CHAM, 2005).

slotted floor was used as outlets (ratio of open air to cover area = 0.18 for fully slotted cover and 0.09 for partially slotted cover). Since it was hard to obtain convergent simulation results when narrow slots (width = 0.03 m) were used as boundary conditions, every set of four of these slots were combined into one larger slot to simplify the simulation boundary condition. However, the slots were uniformly distributed along the tank cover length to represent the real boundary condition. For the circular footprint with the solid cover, the fan was located at the mid-point of the west end, and a square-shaped outlet (L × W = 1 × 1 m) was located at the top edge of the east end. In order to perform high-quality CFD simulations, grid-dependence studies were conducted for each simulation case based on the protocols developed for validating the CFD modeling protocols (Zhao et al., 2007b). In table 1, the grid density (cell number and volume) in each coordinate direction of the simulated tanks is listed. Finer grid density was used in the fan area to ensure simulation accuracy in the area with a high velocity gradient.

The initial and boundary conditions for the simulations of H_2S concentration decrease during forced ventilation were initial concentration (C_0), gas concentration in inlet air (C_{in}, inter-contamination), and gas emission rate from manure surface (ER). In this research, the CFD model was used to simulate the unsteady-state H_2S concentration decrease during forced ventilation to identify the time taken to reach the OSHA permissible exposure limit of 10 ppm for H_2S (T_{pel}) and the time taken to reach 25% of the initial concentration. Momentum effects were much greater than buoyancy effects within the fan-ventilated, confined-space manure tank in this study. In addition, the difference between the outside air temperature and the air temperature in the tank was neglected. Therefore, for the CFD model, the gas (i.e., H_2S) was assumed incompressible with constant density.

The effect of pollutant source on ventilation effectiveness was investigated by conducting simulations for the 12.2 m long rectangular manure tank with the partially slotted cover for pollutant source strengths (emission rate, ER) of $0.65 \times \exp[-0.009 \times t\ (s)]$ mg s^{-1} and 0 mg s^{-1}. The non-zero emission rate under air re-circulation state was reported by Zhao et al. (2007a). The effect of inter-contamination on ventilation effectiveness was investigated by conducting simulations for the 12.2 m long rectangular manure tank with the partially slotted cover for inter-contamination ratios of 0.28 and 0. The high value is the measured value reported by Zhao et al. (2007a) for the partially slotted cover. The effects of manure tank aspect ratio and size on ventilation effectiveness were studied by conducting simulations for rectangular manure tanks with three different lengths and circular manure tanks with two different diameters. The effect of air exchange rate on ventilation effectiveness was studied by conducting simulations at three air exchange rates (1, 3, and 5 AC min^{-1}) for the rectangular tanks with lengths of 5.49 and 12.2 m and for the circular tank with diameter of 6.5 m.

Results

Confined-Space Rectangular Manure Tanks

Effects of Pollutant Source and Inter-Contamination on Gas Removal

Simulations for identifying the effects of pollutant source and inter-contamination on gas removal were performed in the 12.2 m long rectangular storage for the partially slotted cover case at the high air exchange rate (5 AC min^{-1}). Figure 2 shows the comparisons of simulated T_{pel} values at coordinates (X:Y:Z = 0.61:1.37:1.37 m, the origin of the coordinate is shown in fig. 1a) between the manure tank with no pollutant source (ER = 0) and the tank with a pollutant source (ER ≠ 0). Here, the inter-contamination through the fan intake was not included. The comparison shows that including the

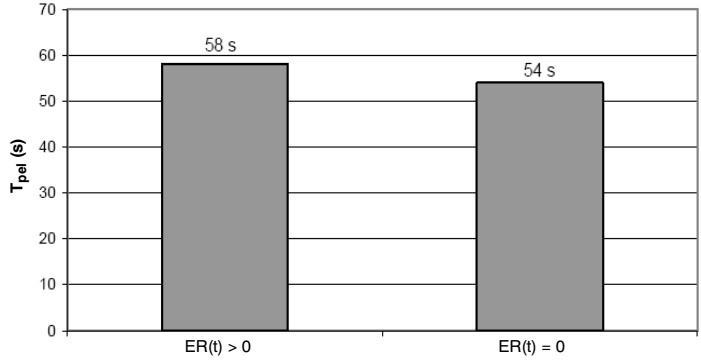

Figure 2. Simulated T_{pel} values at *X*:*Y*:*Z* = 0.61:1.37:1.37 m for the partially slotted cover case with and without pollutant source at the high air exchange rate (C_0 = 110.7 ppm, 5 AC min^{-1}, ER = emission rate).

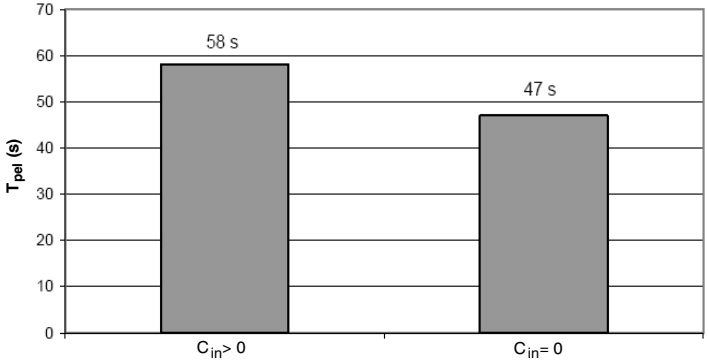

Figure 3. Simulated T_{pel} values at *X*:*Y*:*Z* = 0.61:1.37:1.37 m for the partially slotted cover case with and without intake pollutant source at the high air exchange rate (C_0 = 110.7 ppm, 5 AC min^{-1}, C_{in} = inter-contamination ratio).

pollutant source increased the time taken to reduce the initial H_2S concentration of 110.7 ppm to the OSHA PEL level (10 ppm) by less than 10%. Figure 3 shows the comparisons of simulated T_{pel} values at the same coordinates between the manure tank with and without inter-contamination (ER = 0). The comparison shows that the cross-contamination at the fan intake increased the time taken to reduce H_2S concentration to OSHA PEL level. Compared to the case without pollutant source, the effect of typical inter-contamination strength on the H_2S evacuation time has greater influence on evacuation times (difference = 19%) than does a typical range of H_2S emission rates (difference = 7%).

The comparisons shown in figures 2 and 3 indicate that the gas emission rate and the inter-contamination ratio were two important boundary conditions that contribute to an increase of T_{pel}. Thus, including non-zero gas emission rates and inter-contamination ratios in CFD modeling protocols always yields conservative higher T_{pel} values in simulation results compared to no emission rates and zero inter-contamination ratios. These two boundary conditions were considered and included in the CFD simulations studies for identifying effects of aspect ratio of manure storages and air exchange rate on the evacuation of the H_2S from the confined-space manure tanks.

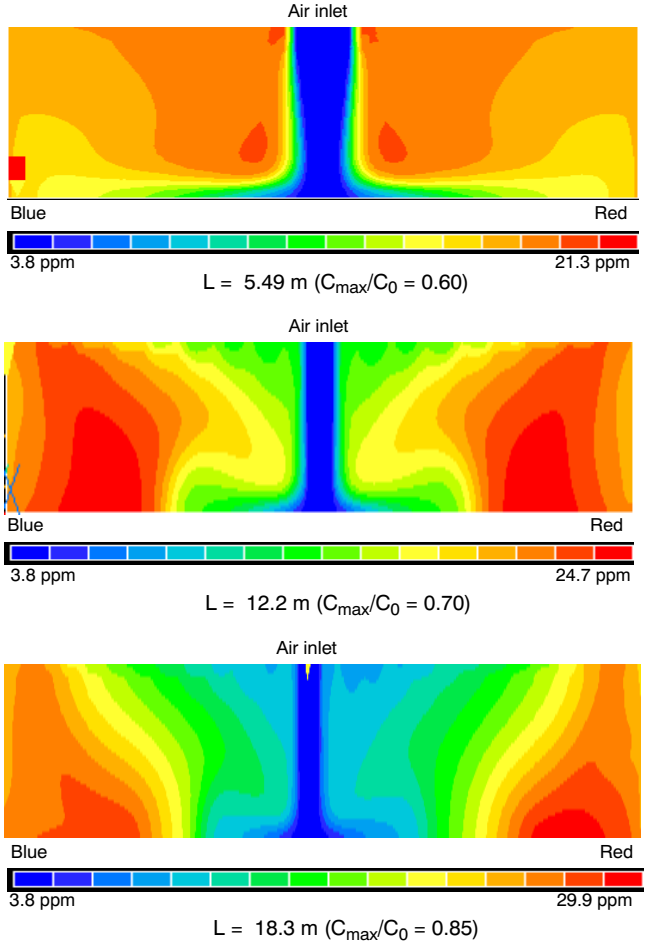

(a) Fully slotted cover (C_0 = 35.3 ppm)

Figure 4. H_2S concentration contours along longitudinal center line 20 s after commencement of ventilation for the fully slotted and the partially slotted cover types (continued on next page).

Effect of Manure Tank Length on Gas Removal

Figures 4a and 4b show, respectively, for the fully slotted cover case ventilated at 3 AC min^{-1} and the partially slotted cover case ventilated at 5 AC min^{-1}, the H_2S concentration contours in the plane along the longitudinal centerline of the 5.49, 12.2, and 18.3 m long simulated rectangular manure tanks 20 s after ventilation commenced. The red color represents the highest gas concentration, and the dark blue color represents the lowest gas concentration for each case. Even though the contour picture for each case has the same size in figure 4, the actual length of the computing domains are different (5.49, 12.2, and 18.3 m) in the longitudinal direction. The simulated results suggest that high-concentration zones (less effectively ventilated zones) exist in the regions closest to the end-walls in the longitudinal direction when the tank length extended to 12.2 m. Figure 5 shows the velocity profiles in the confined airspace along the longitudinal centerline for the fully slotted and partially slotted cover types. From the figure, airflow near the fan

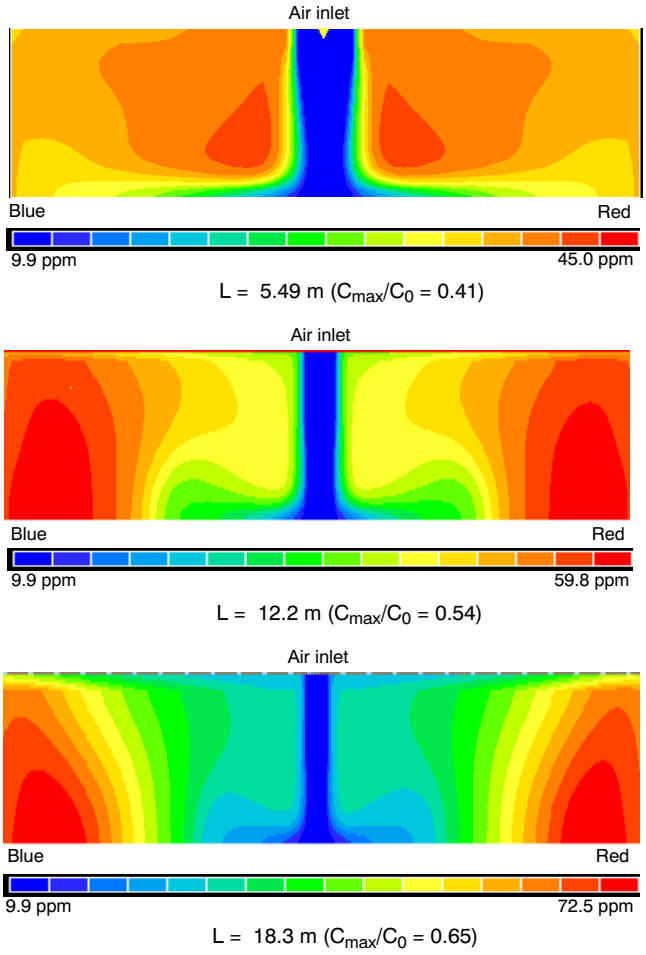

(b) Partially slotted cover (C_0 = 110.7 ppm)

Figure 4 (continued from previous page). H_2S concentration contours along longitudinal center line 20 s after commencement of ventilation for the fully slotted and the partially slotted cover types.

was characterized as increasingly turbulent flow. As length increased, the subsequent loss of momentum caused air velocity profiles in the region farthest from the fan to be less affected by the fan. This explains the high gas concentration zone in the vicinity of the end-walls in the longitudinal direction. The simulated results suggest that the concentration level in the confined airspace increases as the manure tank length increases for the same air exchange rate. For example, for the fully slotted cover case, at the ventilation time of 20 s, the ratio of the maximum concentration level (C_{max}) to the initial concentration level (C_0) for the lengths of 5.49, 12.2, and 18.3 m was 0.60, 0.70, and 0.85, respectively.

Figures 6a and 6b, respectively, show the maximum simulated T_{25} values versus the manure tank length for the fully slotted and partially slotted covers, respectively. The air exchange rate (3 AC min^{-1} for the fully slotted cover type, and 5 AC min^{-1} for the partially slotted cover type) was kept constant for each cover type as length changed. Here, T_{25}

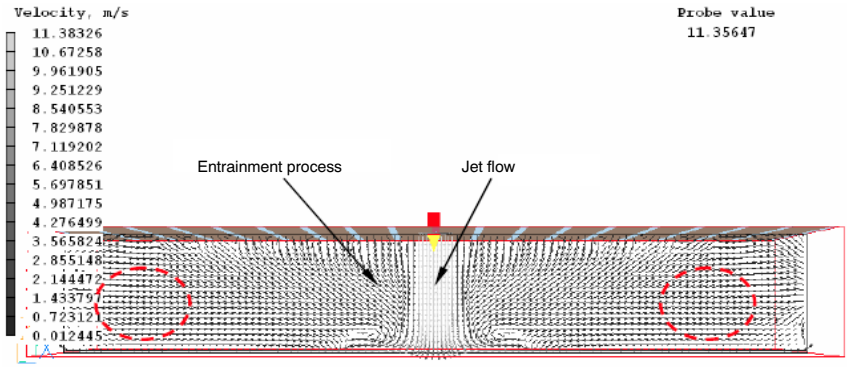

(a) Fully slotted cover

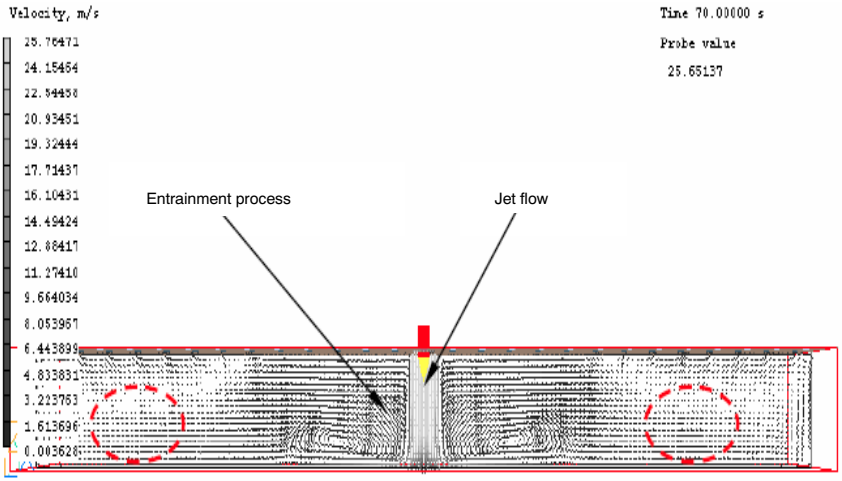

(b) Partially slotted cover

Figure 5. Velocity profiles along longitudinal centerline (L = 12.2 m).

represents the time taken to reach 25% of the initial concentration during forced ventilation. Since the simulations were performed for two cover cases with different initial concentration, comparison of T_{25} values, rather than T_{pel} values, would tend to normalize the effects of different initial concentrations. A linear equation ($T_{25} = a \times$ length + b) was regressed to express the relationship between the maximum simulated T_{25} and the manure tank length. The values of coefficients (a, b) in the regression equation, the standard errors of the coefficients, and P-values are shown in figure 6. There is a statistically significant linear relationship between T_{25} and length at the 90% level. Figure 6 indicates that the time taken to reach 25% of the initial concentration increases linearly with length for each case, provided that AC rate, tank depth, and tank width remain constant. The results show that the time taken to reduce H_2S concentration to 25% of the initial concentration depended on the size of the confined-space storage tank when the same air exchange rate was used.

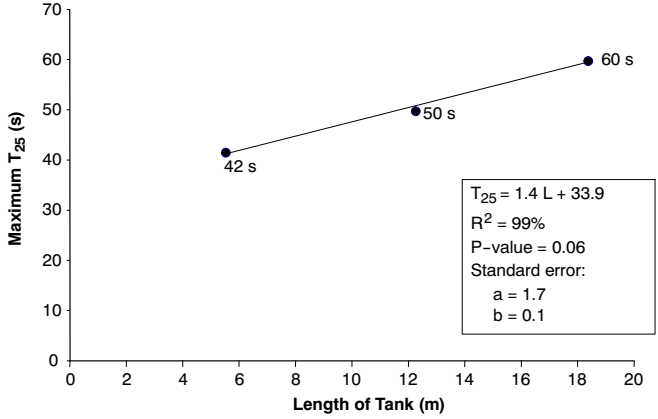

(a) Fully slotted cover

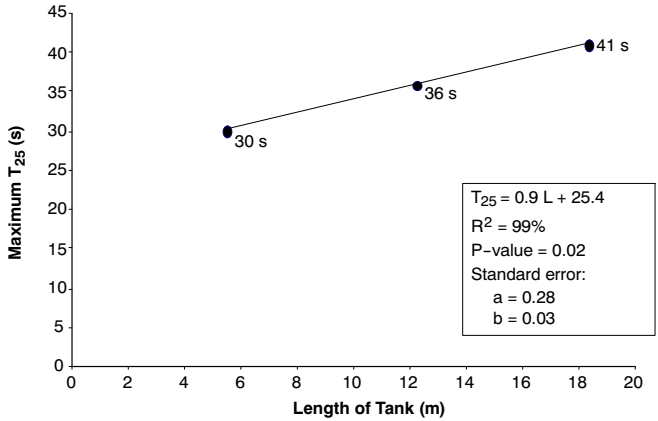

(b) Partially slotted cover

Figure 6. Maximum T_{25} vs. manure storage length values for the fully slotted and the partially slotted cover cases.

Effect of Air Exchange Rate on Gas Removal

The CFD simulations were performed for three air exchange rates (1, 3, and 5 AC min^{-1}) for two tank lengths (5.49 and 12.2 m) for the fully slotted and the partially slotted cover cases. Since the initial concentration was different between the fully slotted and the partially slotted cover cases, the time taken to reduce H_2S concentration to 25% of the initial concentration (T_{25}) and T_{pel} were used to present the relationship between gas evacuation and air exchange rate for two cover types. Figures 7a and 7b, respectively, show the simulated H_2S concentration contours in the plane along the longitudinal centerline of the tanks with the fully slotted and partially slotted covers 20 s after ventilation commenced for the three air exchange rates for two tank lengths (5.49 and 12.2 m). As in figure 4, the red color represents the highest gas concentration, and the dark blue color represents the lowest gas concentration (fan jet region). The simulation results (ratio of the maximum concentration level to the initial concentration level) suggest that increasing the air exchange rate in confined space accelerates the removal of H_2S for the

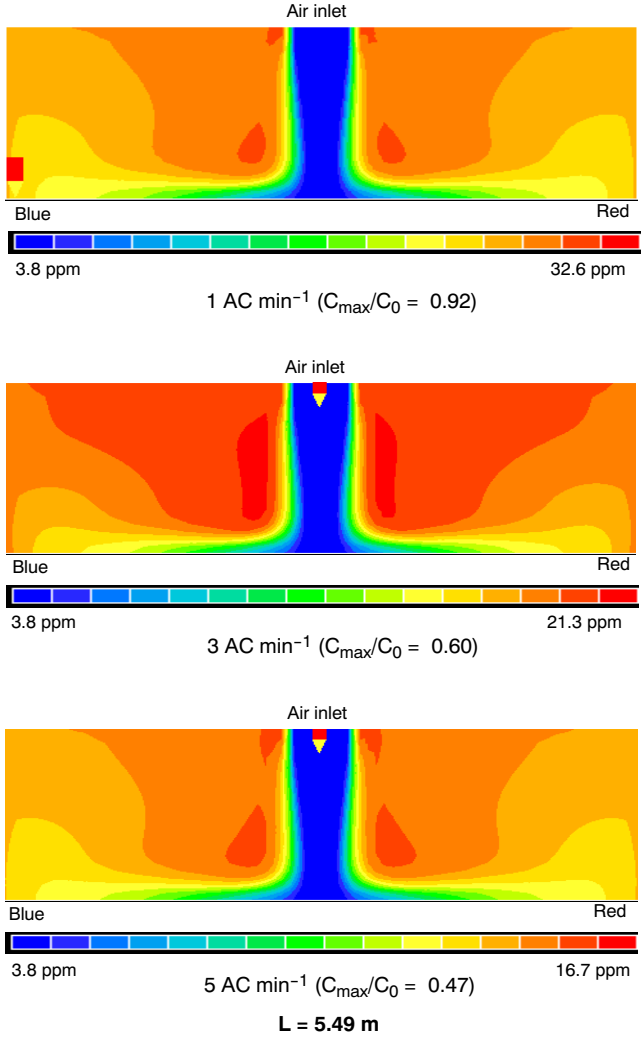

Figure 7. Simulated H_2S concentration contours for the fully slotted and the partially slotted cover cases at the air exchange rates of 1, 3, and 5 AC min^{-1} (continued on next page).

fully slotted and the partially slotted cover cases. For example, for the fully slotted cover case, the ratio of the maximum concentration level to the initial concentration level was 0.92, 0.60, and 0.47 for three air exchange rates, respectively, for the 5.49 m tank.

Figures 8a and 8b show the simulated T_{25} values at locations (X:Y:Z = 1.68:1.37:1.37 m, and X:Y:Z = 2.75:1.00:0.46 m) in the most ineffectively ventilated zone of a 5.49 m long tank for the fully slotted and the partially slotted cover cases and for the three air exchange rates, respectively. Here, the most ineffectively ventilated zone was determined based on gas concentration distribution within the confined space. It represented the zone where the gas concentration level was highest in the confined space. A non-linear relationship between T_{25} value and air exchange rate was identified from the simulated results (fig. 8) for the two cover cases. A power equation ($T_{25} = a \times (\text{AC rate})^b$) was used

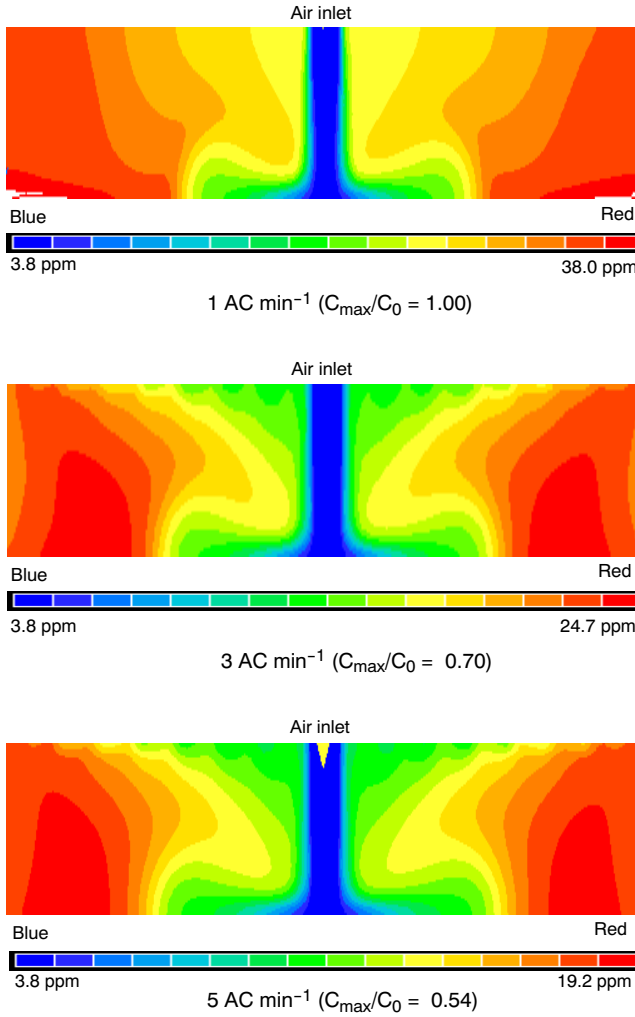

(a) Fully slotted cover (C_0 = 35.3 ppm)

Figure 7 (continued from previous page). Simulated H_2S concentration contours for the fully slotted and the partially slotted cover cases at the air exchange rates of 1, 3, and 5 AC min^{-1}.

to describe the relationship between the maximum T_{25} and air exchange rate (eq. 1). The coefficient of determination (R^2) of the regression model and the standard deviation (s) of residuals of the regression model are listed in figure 8. To compare the regressed results to the simulated results, the average relative difference (ARD, eq. 2) (Bock et al., 1991) was used:

$$T_{25} = 97.8 \times AC^{-0.76} \quad (1a)$$

$$T_{25} = 69.9 \times AC^{-0.74} \quad (1b)$$

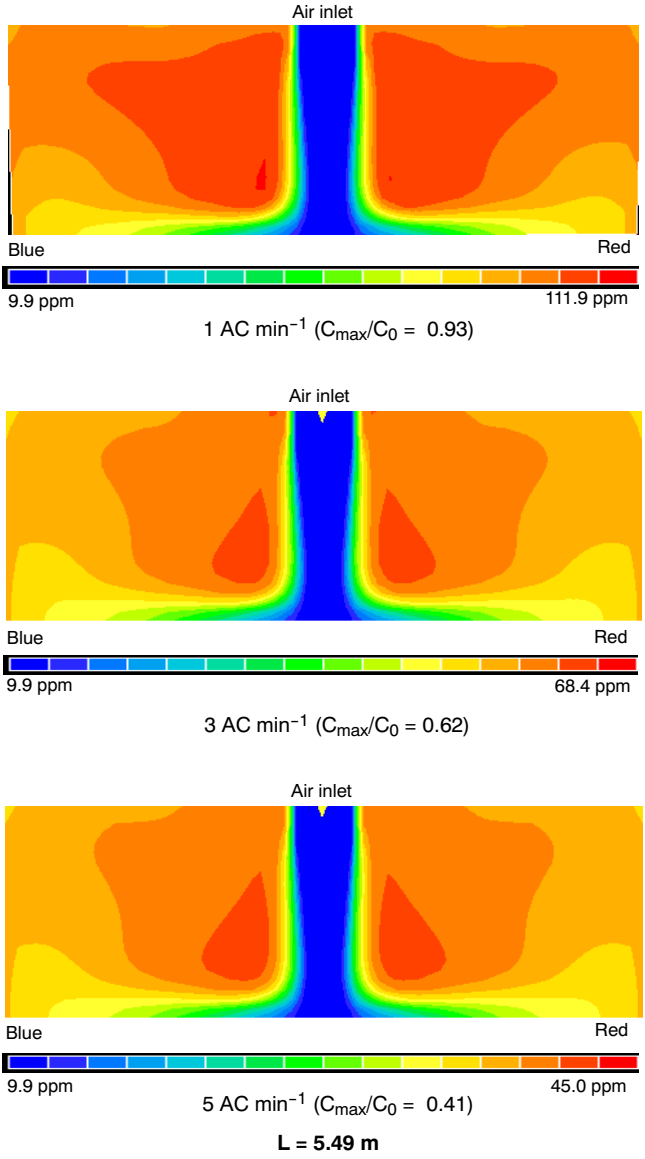

Figure 7 (continued from previous page). Simulated H_2S concentration contours for the fully slotted and the partially slotted cover cases at the air exchange rates of 1, 3, and 5 AC min^{-1}.

$$\text{ARD}\ (\%) = \frac{1}{n}\left[\sum_{i=1}^{n} \frac{\left|regressed\ \ value_i - simulated\ \ value_i\right|}{regressed\ \ value_i} \times 100\right] \quad (2)$$

where

T_{25} = simulated time taken to reduce H_2S concentration to 25% of initial concentration (s)

AC = air exchange rate (AC min^{-1})

n = number of data points.

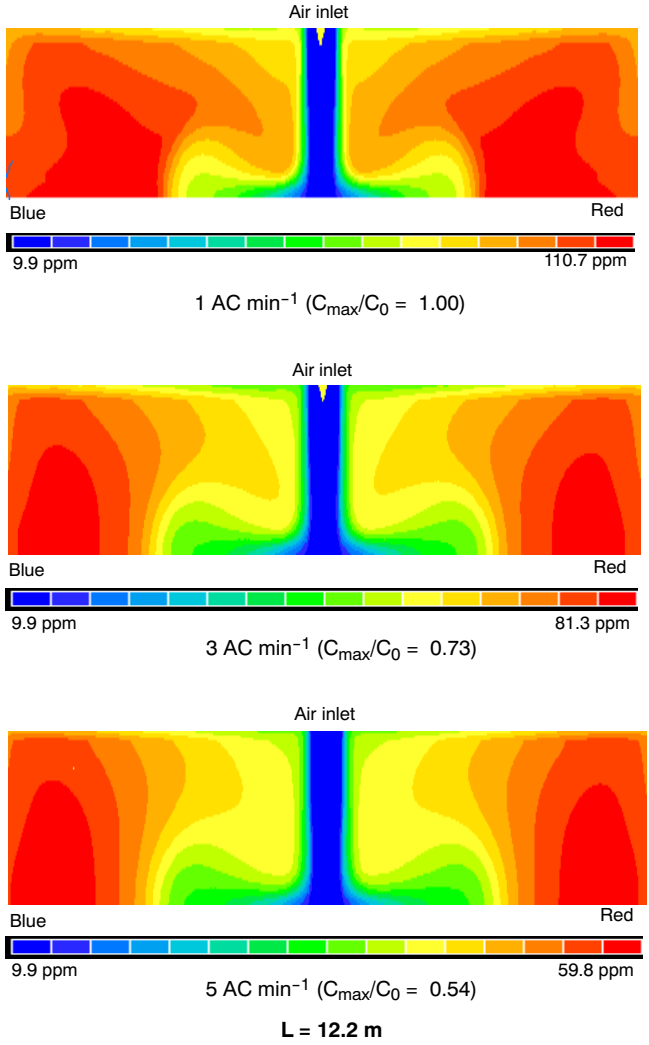

(b) Partially slotted cover (C_0 = 110.7 ppm)

Figure 7 (continued from previous page). Simulated H_2S concentration contours for the fully slotted and the partially slotted cover cases at the air exchange rates of 1, 3, and 5 AC min^{-1}.

The average relative difference between the regressed T_{25} and the simulated T_{25} for the fully slotted cover case was 2.4%. For the partially slotted cover case, the average relative difference between the regressed and the simulated values was 2.4%. The small ARD indicates the small difference between the regressed results and the simulated results for both the fully slotted and the partially slotted cover cases. The regression model reflected the simulated trend of T_{25} with the air exchange rate. The simulated T_{25} values estimated by the resulting regression equation (eq. 1) for two other air exchange rates (2 and 4 AC min^{-1}) were 58 and 34 s for the fully slotted cover case and 42 and 25 s for the partially slotted cover case. The trend in T_{25} with AC rate shows a diminishing rate of gas decay benefit for increasing ventilation rates. For example, for the fully slotted

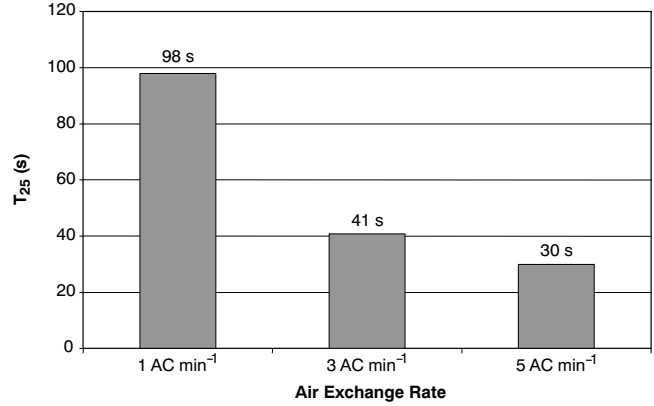

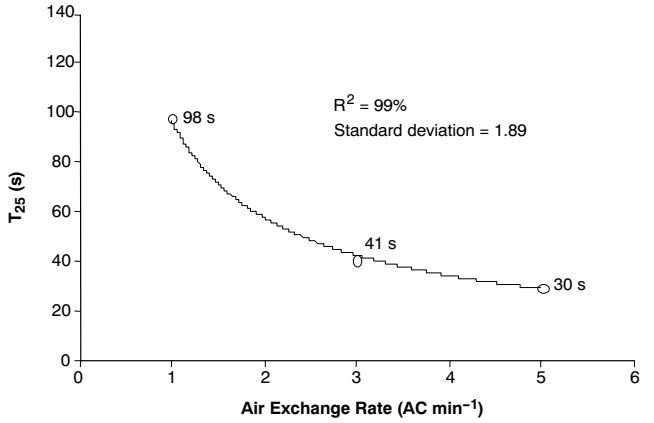

(a) Fully slotted cover

Figure 8. Simulated T_{25} values for three air exchange rates for the fully slotted and the partially slotted cover cases (L = 5.49 m) (continued on next page).

cover case, an increase in ventilation rate from 1 to 3 AC min^{-1} decreased T_{25} by 58% (98 to 41 s), whereas a similar increase in ventilation rate from 3 to 5 AC min^{-1} only decreased T_{25} by 27% (41 to 30 s).

Figures 9a and 9b show the simulated T_{25} values at locations (X:Y:Z = 1.68:1.37:1.37 m, and X:Y:Z = 3.82:1.37:0.46 m) in the most ineffectively ventilated zone of a 12.2 m long storage for the fully slotted and the partially slotted cover cases for three air exchange rates. The power equation of the air exchange rate ($T_{25} = a \times (\text{AC rate})^b$) was identified from the simulated results and used to describe the relationship between simulated T_{25} values and the air exchange rate in the confined-space manure tank for two cover cases (eq. 3):

$$T_{25} = 131.9 \times AC^{-0.84} \quad (3a)$$

$$T_{25} = 92.9 \times AC^{-0.79} \quad (3b)$$

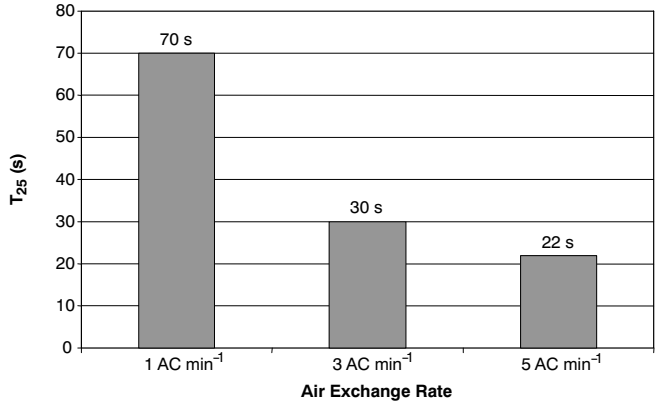

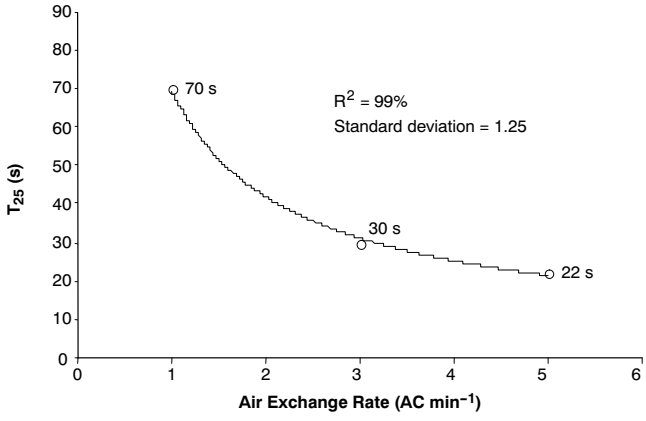

(b) Partially slotted cover

Figure 8 (continued from previous page). Simulated T_{25} values for three air exchange rates for the fully slotted and the partially slotted cover cases (L = 5.49 m).

where T_{25} is the simulated time taken to reduce H_2S concentration to 25% of initial concentration (s), and AC is the air exchange rate (AC min^{-1}).

Based on statistical analysis, the coefficient of determination of the regression model and the standard deviation (s) of residuals of the regression model are shown in figure 9. For the fully slotted cover case, the average relative difference (eq. 2) between the regressed T_{25} and the simulated T_{25} was 1.3%. The ARD for the partially slotted cover case between the regressed and the simulated T_{25} was 2.2%. The small ARD values for the fully slotted and the partially slotted cover cases indicate the small difference between the regressed results and the simulated results. The simulated T_{25} values at the air exchange rates of 2 and 4 AC min^{-1} estimated using the regression equations (eq. 3) were 74 and 41 s for the fully slotted cover case and 54 and 31 s for the partially slotted cover case. The trend in T_{25} with AC rate shows a diminishing rate of gas decay benefit for increasing ventilation rates for the fully slotted and partially slotted cover cases. For example, for the fully slotted cover case, an increase in ventilation rate from 1 to 3 AC min^{-1} decreased T_{25} by 61% (132 to 52 s), whereas a similar increase in ventilation rate from 3 to 5 AC min^{-1} decreased T_{25} by only 33% (52 to 35 s).

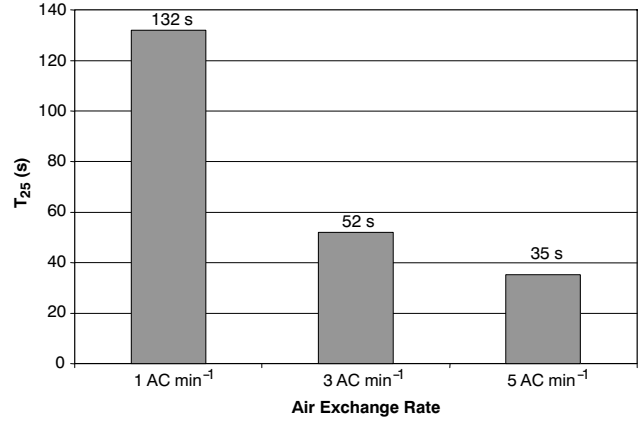

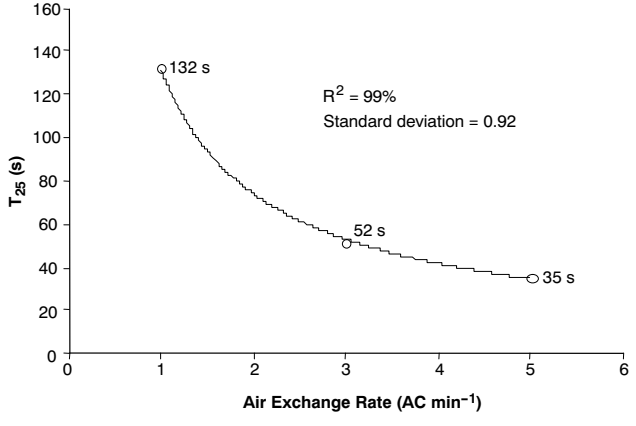

(a) Fully slotted cover

Figure 9. Simulated T_{25} values for three air exchange rates for the fully slotted and the partially slotted cover cases (L = 12.2 m) (continued on next page).

Figures 10a and 10b show the simulated T_{pel} values at locations (X:Y:Z = 1.68:1.37:1.37 m, and X:Y:Z = 2.75:1.00:0.46 m) in the most ineffectively ventilated zone of a 5.49 m long tank for the fully slotted and the partially slotted cover cases and for three air exchange rates, respectively. A non-linear relationship between T_{pel} value and air exchange rate (i.e., $T_{pel} = a \times (\text{AC rate})^b$) was identified as well from the simulated results for the two cover cases. The power equation was used to describe the relationship between maximum T_{pel} and air exchange rate (eq. 4):

$$T_{pel} = 86.5 \times AC^{-0.72} \quad (4a)$$

$$T_{pel} = 136.6 \times AC^{-0.70} \quad (4b)$$

where T_{pel} is the simulated time taken to reduce H_2S concentration to OSHA PEL (s), and AC is the air exchange rate (AC min^{-1}).

The coefficient of determination and the standard deviation of residuals of the regression model are listed in figure 10. The average relative difference between the

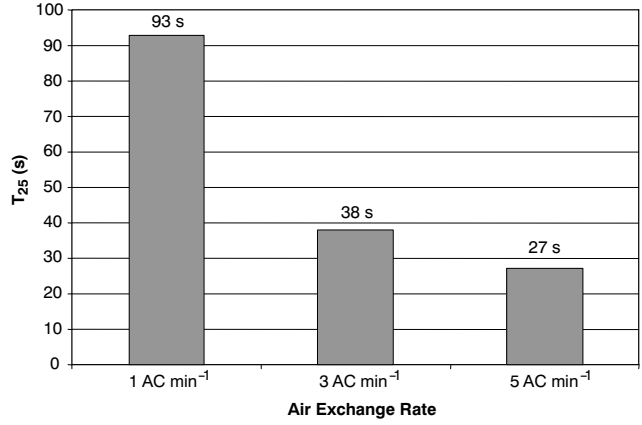

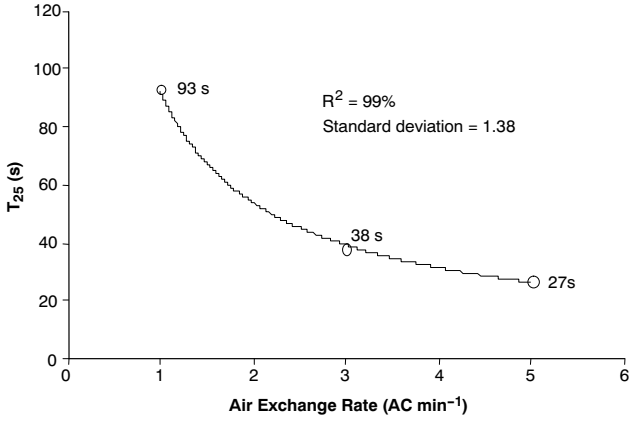

(b) Partially slotted cover

Figure 9 (continued from previous page). Simulated T_{25} values for three air exchange rates for the fully slotted and the partially slotted cover cases (L = 12.2 m).

regressed T_{pel} and the simulated T_{pel} for the fully slotted cover case was 3.7%. For the partially slotted cover case, the average relative difference between the regressed results and the simulated results was 3.4%. The small ARD value of T_{pel} indicates the small difference between the regressed results and the simulated results for both the fully slotted and the partially slotted cover cases. The trend in T_{pel} with AC rate shows a diminishing rate of gas decay benefit for increasing ventilation rates. For example, for the fully slotted cover case, an increase in ventilation rate from 1 to 3 AC min^{-1} decreased T_{pel} by 58% (88 s to 37 s), whereas a similar increase in ventilation rate from 3 to 5 AC min^{-1} only decreased T_{pel} by 24% (37 s to 28 s).

In equations 1 and 3, the constant coefficient of each equation represents the magnitude of the simulated T_{25} value at an AC rate of 1, and the power (e.g., –0.76 and –0.84 for the fully slotted cover case, –0.74 and –0.78 for the partially slotted cover case) determines the rate of decrease in T_{25} with AC rate. The difference in the power values of the two equations is within 10% for both the fully slotted and the partially slotted cover cases. This suggests the same rate of decrease in time of gas decay with AC rate for the

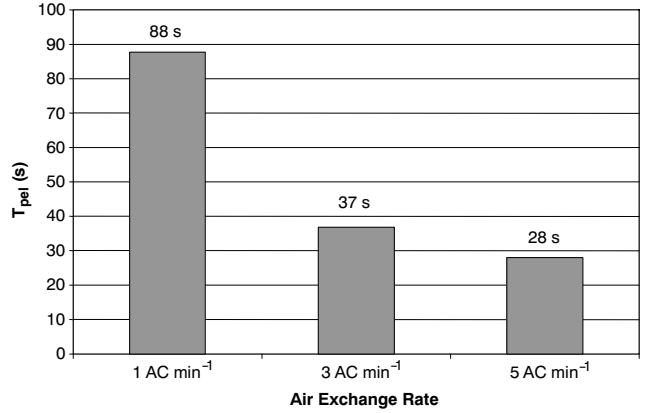

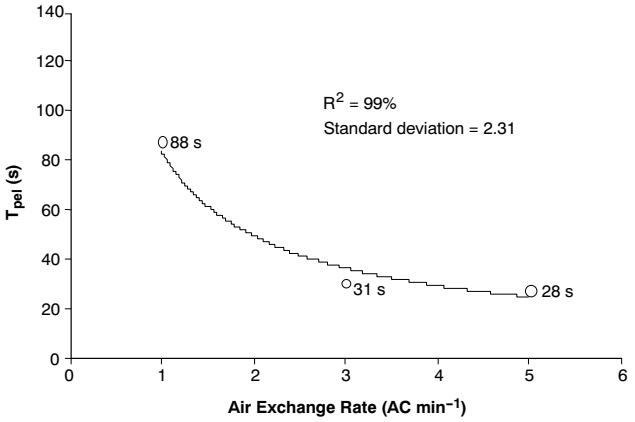

(a) Fully slotted cover

Figure 10. Simulated T_{pel} values for three air exchange rates for the fully slotted and the partially slotted cover cases (L = 5.49 m) (continued on next page).

two tank lengths for the fully slotted and the partially slotted cover cases. Additionally, for the 5.49 m long tank, the power values (–0.76 vs. –0.75 for the fully slotted cover case, –0.74 vs. –0.72 for the partially slotted cover case) of equations 1 and 4 agree to within 10%. This suggests the same rate of decrease in T_{25} and T_{pel} of gas decay for both cover types.

Confined-Space Circular Manure Tanks

Effects of Manure Tank Diameter on Gas Removal

The simulations were performed for the circular manure tanks (solid cover) with diameters of 4.4 and 6.5 m at the air exchange rate of 3 AC min^{-1} to investigate the effect of manure tank diameter on gas removal. Figure 11 shows the simulated H_2S concentration contours at t = 50 s in the X-Y plane 0.25 m above the manure surface and in the X-Z plane through the diameter for the circular manure tanks with diameters of 6.5 and 4.4 m. The initial concentration of H_2S within the confined space was 25 ppm. In figure 11, the red color represents the highest concentration, and the dark blue color represents the lowest concentration. The simulation results suggest that high gas

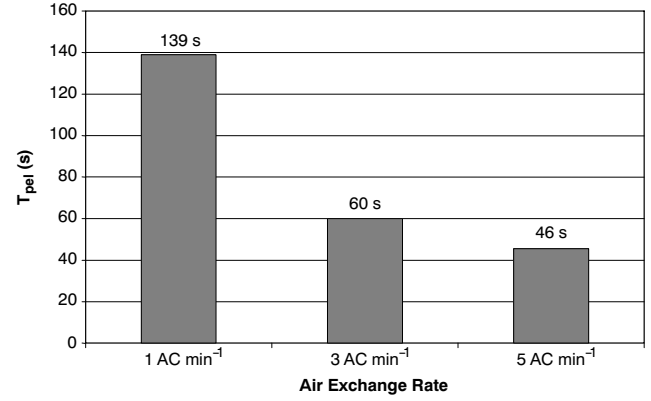

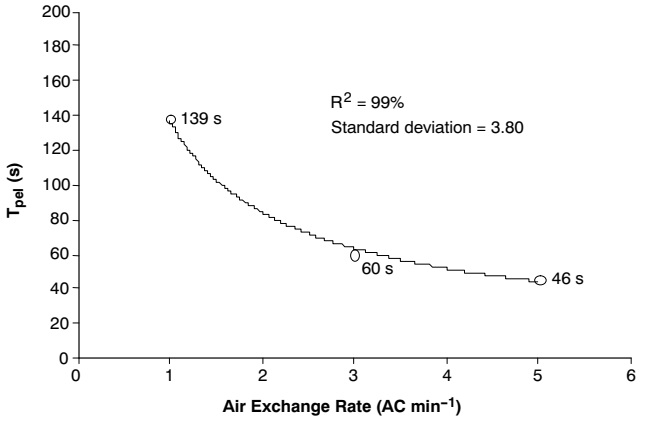

(b) Partially slotted cover

Figure 10 (continued from previous page). Simulated T_{pel} values for three air exchange rates for the fully slotted and the partially slotted cover cases (L = 5.49 m).

concentration zones (the most ineffectively ventilated zones) exist in the regions closest to the wall near the outlet location (fig. 1c). Since the same initial concentration was used in simulations, the time taken to reduce H_2S concentration to the OSHA PEL level (10 ppm) (T_{pel}) was used to present gas evacuation. Figure 12 shows the simulated T_{pel} values at locations *X*:*Y*:*Z* = 4.0:2.2:1.4 m (D = 4.4 m) and *X*:*Y*:*Z* = 6.0:3.3:1.4 m (D = 6.5 m), both of which were located at the mid-point of the outlet boundary surface (*X*-*Y* direction) 0.46 m below the outlet. These locations were in the zone of the highest simulated gas concentration and were near the only possible personnel entrance into the circular manure tanks simulated in this study. As the diameter increased by 32% (4.4 to 6.5 m), the T_{pel} values at the selected location increased by approximately 37%. The simulated results suggest that the maximum time to evacuate H_2S from the confined space increased with tank diameter when ventilated at the same AC rate.

Effects of Air Exchange Rate on Gas Removal

The simulations were performed for the circular manure tank with diameter of 6.5 m for three air exchange rates (1, 3, and 5 AC min^{-1}) to identify the trend between air exchange rate and gas removal. Figure 13 shows the simulated H_2S concentration

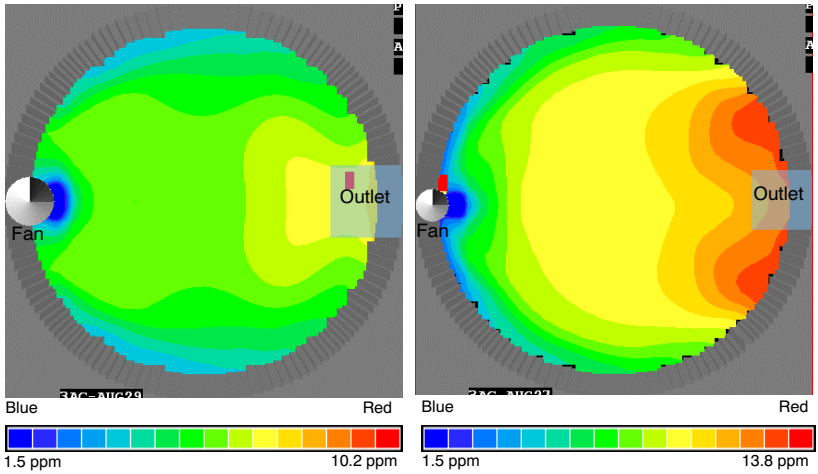

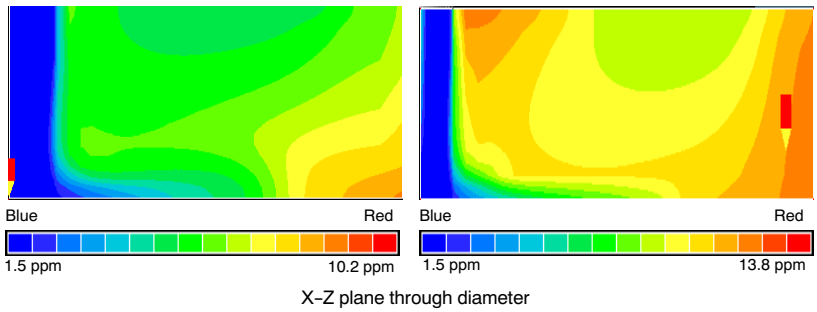

(a) D = 4.4 m (C_{max}/C_0 = 0.41) **(b) D = 6.5 m (C_{max}/C_0 = 0.55)**

Figure 11. Simulated H_2S concentration contours for the circular manure tanks at the air exchange rate of 3 AC min^{-1} for diameters of 4.4 and 6.5 m (C_0 = 25 ppm).

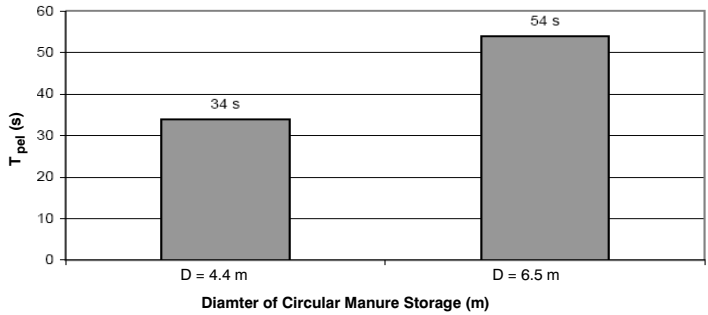

Figure 12. Simulated T_{pel} values for two circular manure tanks at locations X:Y:Z = 4.05:2.2:1.37 m (D = 4.4 m) and X:Y:Z = 6.05:3.25:1.37 m (D = 6.5 m) below the outlet at the air exchange rate of 3 AC min^{-1}.

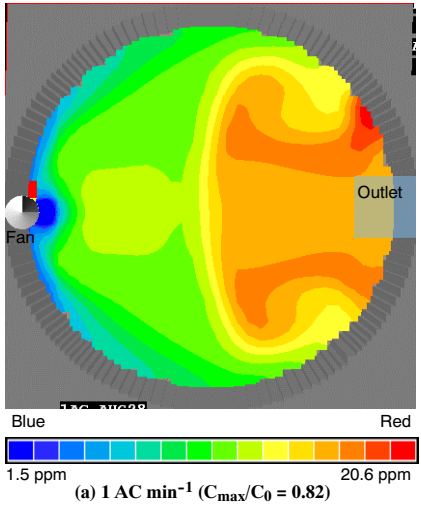

(a) 1 AC min^{-1} (C_{max}/C_0 = 0.82)

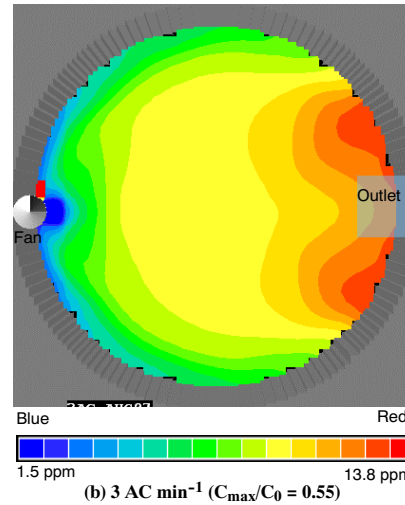

(b) 3 AC min^{-1} (C_{max}/C_0 = 0.55)

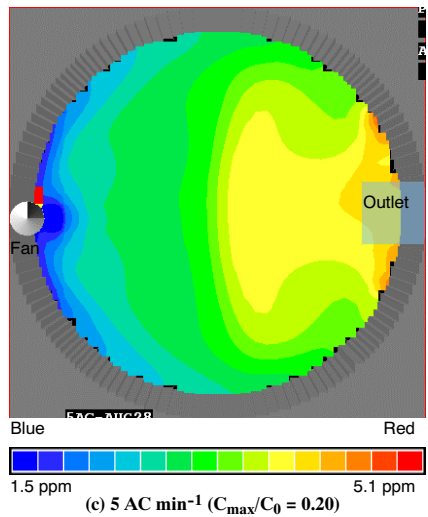

(c) 5 AC min^{-1} (C_{max}/C_0 = 0.20)

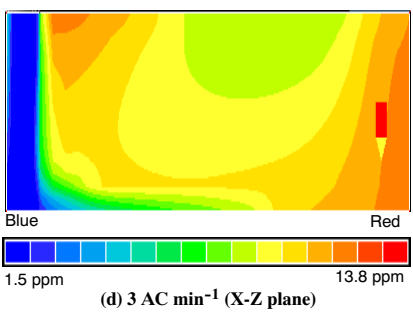

(d) 3 AC min^{-1} (X-Z plane)

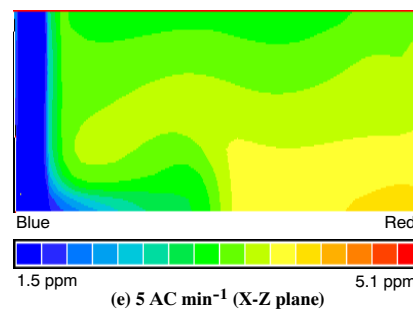

(e) 5 AC min^{-1} (X-Z plane)

Figure 13. Simulated H_2S concentration contours for the circular manure tank at (a) 1 AC min^{-1}, (b) 3 AC min^{-1}, and (c) 5 AC min^{-1} air exchange rates at 0.25 m above the manure surface and contours of *X-Z* plane through diameter at (d) 3 AC min^{-1} and (e) 5 AC min^{-1} (D = 6.5 m, C_0 = 25 ppm).

contours 0.25 m above the manure surface in the *X-Y* plane at t = 50 s for the 6.5 m diameter circular manure tank. In addition, the simulated H_2S concentration contours of the vertical cross-section (*X-Z* plane) through the diameter along the longitudinal centerline for the air exchange rates of 3 and 5 AC min^{-1} at t = 50 s (the contour at the same location for the air exchange rate of 1 AC min^{-1} was not saved) are also shown in figure 13. The red color represents the highest gas concentration, and the dark blue color represents the lowest concentration. These results show that increasing the air exchange rate in the confined space accelerated the evacuation of H_2S from the circular confined-space manure tanks.

Figure 14 shows the simulated T_{pel} values at a selected location (*X*:*Y*:*Z* = 5.55:3.25:1.37 m) for three air exchange rates (1, 3, and 5 AC min^{-1}). The selected location was at the mid-point of the outlet boundary surface (*X-Y* direction) 0.46 m below the outlet. This location was near the only possible personnel entrance to the circular manure tank and was also the location of the highest gas concentrations during ventilation simulations The results of a regression of evacuation time versus diameter (eq. 5) show that the relationship is linear (P = 0.05):

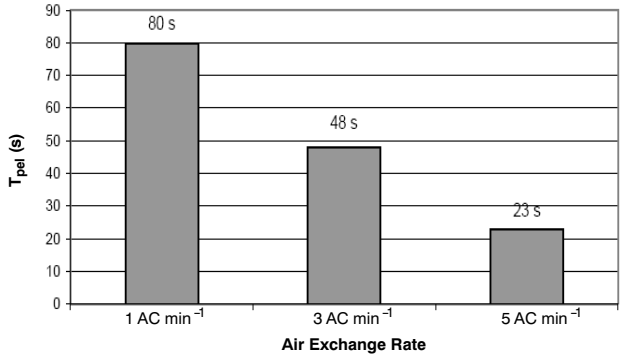

(a) T_{pel} values for three air exchange rates

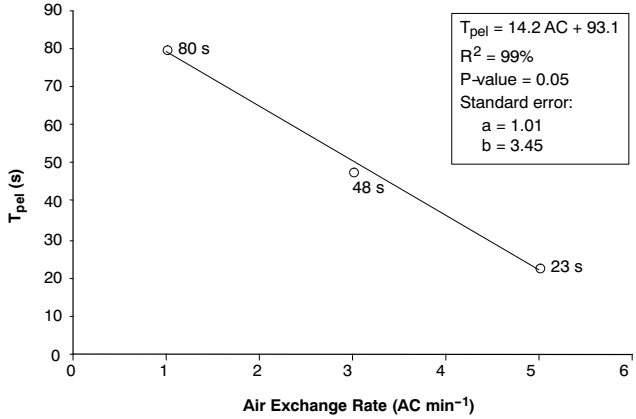

(b) Nearly linear relationship: T_{pel} vs. AC rate

Figure 14. Simulated T_{pel} values for three air exchange rates: 1, 3, and 5 AC min^{-1} for the circular manure tank with diameter of 6.5 m (C_0 = 25 ppm).

$$T_{pel} = -14.2\,AC + 93.1 \quad (5)$$

where T_{pel} is the simulated time taken to reduce H_2S concentration to OSHA PEL level (s), and AC is the air exchange rate (AC min^{-1}).

For example, increasing ventilation rate from 1 to 3 AC min^{-1} decreased T_{pel} by 40% (80 to 48 s), whereas a similar increase in ventilation rate from 3 to 5 AC min^{-1} decreased T_{pel} by 52% (48 to 23 s). The trends in simulated evacuation times with air exchange rate differed between the circular and rectangular manure tanks for the study ventilation configurations. Thus, air exchange rate effects on evacuation times are tank geometry and ventilation configuration dependent.

Conclusions

In this research, validated CFD modeling protocols were used to perform simulations of a range of typical sizes of two types of on-farm manure tank geometries: rectangular and circular. Three air exchange rates (1, 3, and 5 AC min^{-1}) were investigated to identify the effect of the air exchange rate on the H_2S evacuation from the confined space. The effect of the manure tank length (rectangular tanks) or diameter (circular tanks) on the evacuation of the H_2S from the confined space at a given air exchange rate was investigated. In addition, the effects of gas emission rate and inter-contamination strength on the gas evacuation were identified for the rectangular manure tank with the partially slotted cover type at the high air exchange rate (5 AC min^{-1}). The simulation studies for two manure tank geometries lead to the following conclusions:

- For the same air exchange rate, as the length of the rectangular manure tank increased, the rate of evacuation of the H_2S from the confined space, especially in zones far from the ventilating fan, decreased for both the fully slotted and partially slotted cover cases.
- For the rectangular manure tank, the higher the air exchange rate, the higher the rate of evacuation of the H_2S from the confined space. However, the rate of evacuation of the H_2S from the confined space increased at a decreasing rate with AC rate.
- For the rectangular manure tank, the gas emission rate and the inter-contamination strength were identified as two important boundary conditions. Typical ranges of inter-contamination strength had a greater influence on the rate of evacuation of H_2S from the confined space than did a typical range of gas emission rate from the stored manure. Including non-zero gas emission rates and non-zero inter-contamination ratios in the CFD simulation protocols always yielded conservative T_{PEL} or T_{25} evacuation times.
- For the same air exchange rate, as the diameter of a circular manure storage increased, the rate of evacuation of the H_2S from the tank decreased, especially in zones farthest from the fan location, for the solid cover case.
- For the circular manure tank, the higher air exchange rate accelerated the evacuation of the H_2S from the confined space. The relationship between air exchange rate and T_{pel} was nearly linear.
- The relationship between air exchange rate and gas evacuation rate was dependent on tank geometry and ventilation configuration.

Acknowledgements

The authors gratefully acknowledge the Northeast Center for Agricultural and Occupational Health and the National Institutes of Health for funding this research (Project No. 1U50/OH07542).

References

ASAE Standards. 2004. EP393.3: Manure storages. St. Joseph, Mich.: ASAE.

Beaver, R., and W. E. Field. 2007. Summary of documented fatalities in livestock manure storage and handling facilities: 1975-2004. *J. Agromed.* 12(2): 3-23.

Bock, R. G., V. M. Puri, and H. B. Manbeck. 1991. Triaxial test sample size effects on stress relaxation of wheat en masse. *Trans. ASAE* 34(3): 966-971.

CHAM. 2005. PHOENICS Version 3.6. London, U.K.: CHAM, Ltd.

CDC. 1993. Fatalities attributed to entering manure waste pits: Minnesota, 1992. *MMWR* 42(17): 325-329.

Lloyd, W. E. 2000. Ventilation for confined space entry into underground manure storage facilities. MS thesis. University Park, Pa.: The Pennsylvania State University, Department of Agricultural and Biological Engineering.

Murphy, D. J., and S. Steel. 2001. Manure storage hazards. Cooperative Extension Article E28. University Park, Pa.: The Pennsylvania State University.

MWPS. 1987. Swine planning. In *Structures and Environment Handbook*, MWPS-703. Ames, Iowa: Midwest Plan Service.

NIOSH. 1990. NIOSH Alert: Preventing deaths of farm workers in manure pits. Publication No. 90-103. Cincinnati, Ohio: National Institute of Occupational Safety and Health.

OSHA. 1995. Air contaminants, 29 CFR 1910.1000. Washington, D.C.: Occupational Safety and Health Administration.

OSHA. 1998. Permit-required confined spaces, OSHA 3138. Washington, D.C.: Occupational Safety and Health Administration.

OSHA. 2002. Application of the permit-required confined spaces (PRCS), 29 CFR 1910.146. Washington, D.C.: Occupational Safety and Health Administration.

Pesce, E., J. Zhao, H. B. Manbeck, and D. J. Murphy. 2007. Screening ventilation strategies for confined-space manure storages. *J. Agric. Safety and Health* 14(3): 283-308.

Sørensen, D. N., and P. V. Nielsen. 2003. Quality control of computational fluid dynamics in indoor environments. *Indoor Air* 13(1): 2-17.

Zhao, J., H. B. Manbeck, and D. J. Murphy. 2007a. Hydrogen sulfide emission rates and inter-contamination strengths in fan-ventilated confined-space manure storages. *Trans. ASABE* 50(6): 2217-2229.

Zhao, J., H. B. Manbeck, and D. J. Murphy. 2007b. Computation fluid dynamics simulation and validation of H_2S removal from fan-ventilated confined-space manure storages. *Trans. ASABE* 50(6): 2231-2246.